論文 한국정밀공학회지 제14권 제6호 (1997년 6월)
Journal of the Korean Society of Precision Engineering Vol. 14. No. 6. June. 1997.

3차원 균열에 대한 자동화된 응력확대계수해석 시스템 개발

이 준 성*

Development of Automated Stress Intensity Factor Analysis System for Three-Dimensional Cracks

Lee, Joon-Seong*

ABSTRACT

솔리드 모델러, 자동요소분할 기법, 4면체 특이요소, 응력확대계수의 해석 기능을 통합하여, 3차원 균열의 응력확대계수를 효율적으로 해석할 수 있는 시스템을 개발하였다. 균열을 포함하는 기하모델을 CAD 시스템을 이용하여 정의하고, 경계조건과 재료 물성치 및 절점밀도 분포를 기하모델에 직접 지정함으로써, 퍼지이론에 의한 절점발생과 데로우니 삼각화법에 의한 요소가 자동으로 생성된다. 특히, 균열 근방에는 4면체 2차 특이요소를 생성시켰으며, 유한요소 해석을 위한 입력데이터가 자동으로 작성되어 해석코드에 의한 응력 해석이 수행된다. 해석 후, 출력되는 변위를 이용하여 변위외삽법에 의한 응력확대계수가 자동적으로 계산되어 진다. 본 시스템의 효용성을 확인하기 위해, 인장력을 받는 평판내의 표면균열에 대해 해석하여 보았다.

Key Words: Finite Element Analysis (유한요소해석), Stress Intensity Factor (응력확대계수), Surface Crack (표면균열), Automatic Mesh Generation (자동요소분할), Fuzzy Theory (퍼지이론), Bucketing Method (버켓법), Delaunay Triangulation (데로우니 삼각형), Singular Element (특이요소)

Nomenclature

a	a depth of a semi-elliptical surface crack
c	a half length of a semi-elliptical surface crack
d	a distance between two semi-elliptical surface cracks
K_I	the stress intensity factor(SIF) for a Mode I crack
W	a half width of a plate with cracks
t	a plate thickness
Q	a shape factor for a semi-elliptical surface crack
ϕ	a parametric angle of the ellipse
σ	an applied uniform tensile stress
E	Young's modulus
ν	Poisson's ratio
x, y, z	Cartesian coordinates

* 경기대학교 기계공학과

1. Introduction

3D cracks such as surface or embedded cracks are more common flaws being found in practical structures. Analyses of the 3D cracks are desirable in structural integrity studies of practical structures. The SIFs for an elliptical or a semi-elliptical crack have been obtained by the finite element method (FEM)[1-5]. However, there are still some problems to be solved. The main concern for the FEM is a relatively higher computation cost, especially when dealing with 3D crack problems. To overcome this, several techniques such as the direct method[6], the virtual crack extension method[7], the superposition method[8] and the special singular element method[9,10] have been proposed in conjunction with the FEM. It should be also noted here that the data preparation for 3D crack analyses require special element arrangement near the crack front, and that much efforts are necessary to generate such special meshes. Dramatic progress in computer technology now shortens computation time. However in reality, labour intensive tasks to prepare a FE model of a structural component with 3D cracks are still a bottle neck. The author has proposed an automatic FE mesh generation method for 3D structures consisting free-form surfaces[11]. In the present study, by integrating this mesh generator, one of commercial FE analysis codes and some additional techniques to calculate the SIF, a new automated system for analyzing the SIFs of 3D cracks was developed.

To examine accuracy and efficiency of the present system, the SIF for a semi-elliptical surface crack in a plate subjected to uniform tension is calculated and compared with Raju-Newman's solutions[5,12]. Then the system is applied to analyze interaction effects of twin semi-elliptical surface cracks in a plate subjected to uniform tension.

2. Fundamental Principle and Algorithms

The biggest advantage of the present analysis system is a very simple operation to analyze complex structures such as a plate with twin semi-elliptical surface cracks. A flow of analyses using the present system is shown in Fig. 1. Each sub-process will be described below. The details of the mesh generation part can be found[11].

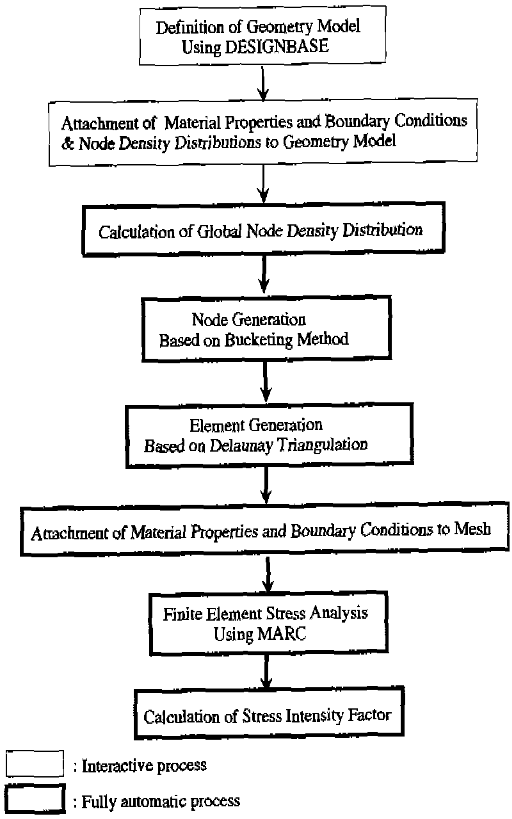

Fig.1 Flow of analysis

2.1 Definition of Geometry Model

A whole analysis domain is defined using one of commercial geometry modelers, DESIGNBASE[13] which has abundant libraries which enable us to easily operate, modify and apply to a solid model. Any information related to a geometry model can be easily retrieved by the libraries of DESIGNBASE.

2.2 Attachment of Material Properties and Boundary Conditions to Geometry Model

Material properties and boundary conditions are directly attached onto the geometry model by clicking the loops or edges that are parts of the geometric model using a mouse, and then by inputting values. The present system deals with displacement as well as force boundary conditions.

2.3 Designation of Node Density Distributions

A node density distribution over a whole geometry model is constructed as follows. The present system stores several local node patterns such as the pattern suitable to well capture stress concentration, the pattern to subdivide a finite and whole domain uniformly. A user selects some of those local node patterns and designates where to locate them. Then a global distribution of node density over the whole analysis domain is automatically calculated through their superposition using the fuzzy knowledge processing [14].

2.4 Node Generation

Node generation is one of time consuming processes in automatic mesh generation. In the present study, the bucketing method[15] is adopted to generate nodes which satisfy the distribution of node density over a whole analysis domain. Fig. 2 shows its fundamental principle, taking the previous two-dimensional mesh generation as an example without any loss of generality. Let us assume that the distribution of node density over a whole analysis domain is already given as shown in Fig. 2(a). At first, a super-rectangle enveloping the analysis domain is defined as shown in Fig. 2(b). In the 3D solid case, a super hexahedron is utilized to envelop an analysis domain. Next, the super-rectangle is divided into a number of small sub-rectangles, each of which is named "Bucket" Nodes are generated bucket by

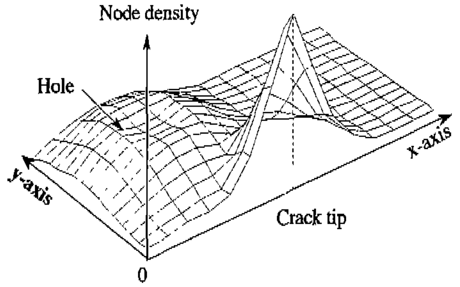

(a) Example of node density distribution

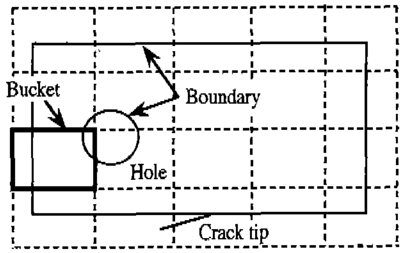

(b) Example of bucket decomposition

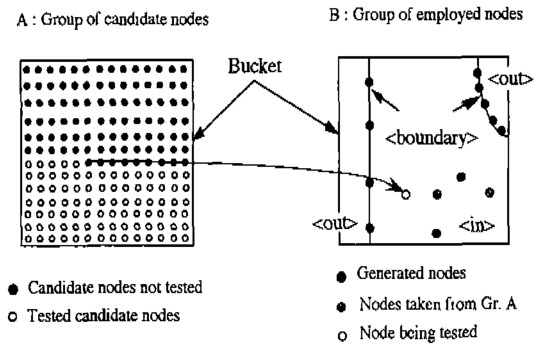

(c) Node generation in one of buckets

Fig.2 Node generation based on bucketing method

bucket.

At first, a number of candidate nodes with uniform spacing are prepared in one of buckets as shown in Fig. 2(c). The distance of two neighboring candidate nodes is set to be smaller than the minimum distance of nodes to be generated in the relevant bucket. Next, candidate nodes are pick up one by one, starting from the left-bottom corner of the bucket, and are put into the bucket. A candidate node is adopted as one of the final nodes when it satisfies the following two criteria :

(a) The candidate node is inside the analysis domain (IN/OUT check).
(b) The distance between the candidate node and the nearest node already generated in the bucket satisfies the node density at the point to some extent.

Practically, the criterion (a) is first examined bucket by bucket. As for buckets lying across the domain boundary, the criterion (a) is examined node by node. It should be noted here that the nodes already generated in the neighboring buckets have to be examined for the criterion (b) as well when a candidate node is possibly generated near the border of the relevant bucket. In the bucketing method, the number of examinations of the criterion (b) can be reduced significantly, and then a node generation speed is remained to be proportional to the total number of nodes. As for 3D solid geometries, nodes are generated in the following order : vertices, edges, surfaces and domain.

2.5 Element Generation

The Delaunay triangulation method[16 17] is used to generate tetrahedral elements from numerous nodes produced within a geometry. When the Delaunay triangulation method is utilized to generate elements in a geometry with cracks, mis-match elements across surface crack front tend to occur as shown in Fig. 3(a). To avoid the mis-

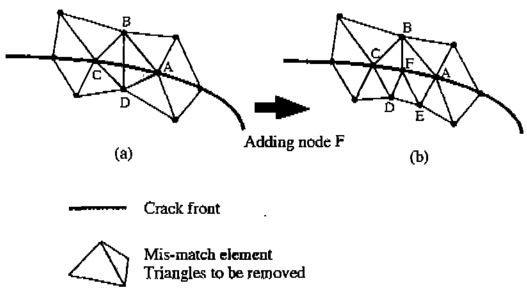

Fig.3 Technique of avoiding mis-match elements

match elements, node densities on the crack front are automatically controlled to be slightly higher than those near the crack as shown in Fig. 3(b).

2.6 Automatic Attachment of Material Properties and Boundary Condiions to FE Mesh

Through the interactive operations mentioned in section 2.2, a user designates material properties and boundary conditions onto the geometry model. Then these are automatically attached on nodes, edges, faces and volume of elements. Such automatic conversion can be performed owing to the special data structure of FEs such that each part of element knows which geometry part it belongs to. Finally, a complete FE model consisting of mesh, material properties and boundary conditions is obtained. The current version of the system produces FEs compatible to quadratic tetrahedral elements implemented in one of the commercial FE codes, MARC.

3. Calculation of SIF

The FE model generated is automatically analyzed using MARC, and then displacements, strains and stresses are calculated. To obtain the SIFs accurately as well as automatically, some techniques are employed.

3.1 Singular Element

When ordinary quadratic tetrahedral elements are employed to calculate the SIF, a very fine mesh is required near crack front to capture $\sqrt{r}$ variation in displacements and $1/\sqrt{r}$ variation in stresses where r denotes the distance from crack front. To relax this situation, singular elements as shown in Fig. 4 are adopted[9 10]. In the singular element, the mid-point nodes near a crack front are shifted to the quarter-points. This conversion of ordinary tetrahedral elements along a front of 3D crack to the singular elements is auto-

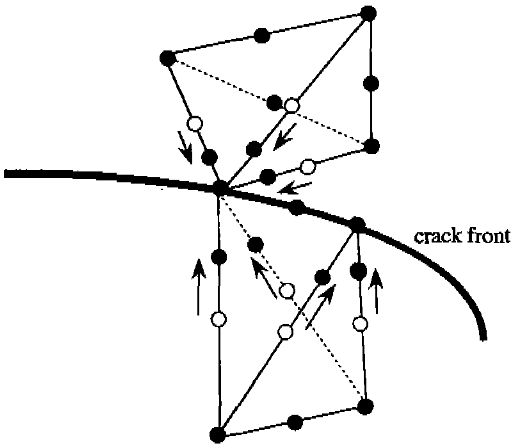

Fig.4 Conversion of ordinary quadratic tetrahedral elements along crack front into singular elements

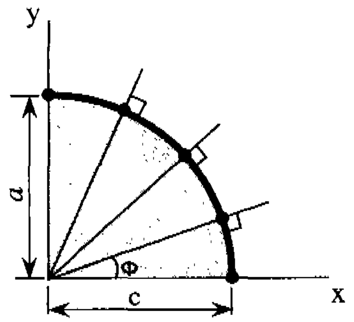

(a) Half semi - circular surface crack(a = c)

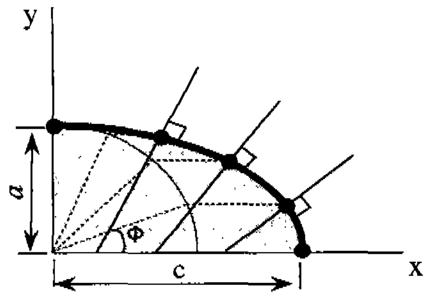

(b) Half semi - elliptical surface crack

Fig.5 Definition of radial lines to calculate the stress intensity factors

matically performed in the last stage of the creation of a FE model.

3.2 Calculation of SIFs

SIFs are computed using the displacement extrapolation method[26]. Nodal displacements calculated along the crack face are substituted in the following crack tip displacement equation :

$$K = \frac{E'}{4}\sqrt{2\pi}\lim_{r\to 0}\frac{w}{\sqrt{r}},$$

$$E' = \begin{cases} \dfrac{E}{1-\nu^2}\,(for\ \ plane\ \ strain) \\ E \quad (for\ \ plane\ \ stress) \end{cases} \tag{1}$$

where w is a nodal displacement, and E′ is equal to E in the plane stress condition or $E/(1-\nu^2)$ in the plane strain condition. Only positions of free surface intersection are regarded as in the plane stress condition, while other positions are in the plane strain condition. Although there is no clear boundary between the plane strain region and the plane stress region, the point on the free surface, i.e. ϕ =0, is in plane stress. Radial lines for the semi-elliptical surface crack front and those of the semi-circular one are defined as in Fig. 5.

For each radial line with an elliptic angle ϕ , the nodal displacements resulting from an FE calculation are inserted in the well-known equation (1) for the displacements near the crack tip. By this means, SIF values K for each radial line may be computed from the displacements of the nodes at distance r from the crack face. The first segment of the K curve where K depends linearly on r is extrapolated to r = 0. The intersection with the K-axis yields the desired value for the SIF. The procedure is rather tedious and a distinct linear segment cannot be recognized in every load case. Therefore, the least square method is applied to evaluate the SIF. In this least square operation, the K value evaluated at the shifted quarter point is neglected. This displacement extrapolation method is popularly used to calculate the SIF. In the present study, this process is fully automated. When a crack is designated by a user in the definition process of a geometry model, radial lines for the crack front are automatically determined. After the stress analysis using MARC, displacement distributions are interpolated along the radial lines, on each of which the SIF is calculated by the least square method.

4. Results and Discussion

4.1 Analysis of Single Surface Crack

In order to examine efficiency and accuracy of the present system, a surface cracked plate of width 2b, thickness t and height 2h subjected to uniform tension as shown in Fig. 6 was analyzed. A semi-elliptical surface crack is assumed here.

Fig. 7 shows a typical FE mesh of a quarter

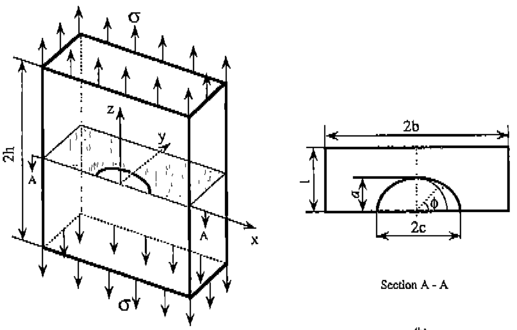

(a) (b)

Fig.6 A plate with a semi-elliptical surface crack subjected to uniform tension

portion of a plate with a semi-elliptical surface crack generated by the present system. The mesh consists of 2,982 quadratic tetrahedral elements and 5,842 nodes. Nodes and elements are generated in about 90 seconds and in about 25 seconds, respectively. This is measured on a popular engineering workstation (EWS), SUN SparcStation 10. To complete this mesh, the following three node patterns are utilized ; (a) the base node pattern in which nodes are generated with uniform spacing over a whole analysis domain, (b) a special node pattern for the semi-elliptical

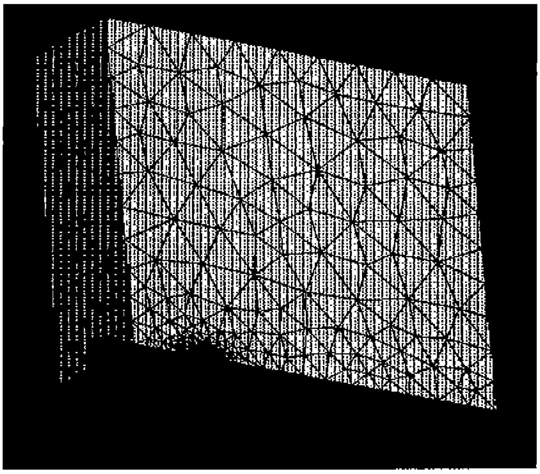

Fig.7 A typical mesh of a quarter portion of a plate with a semielliptical surface crack(2,982 elements, 5,842 nodes)

surface crack, and (c) a special node pattern in which node density is getting coarser departing from the bottom face including the surface crack and the ligament section.

The analyses were performed for three aspect ratios of a/c = 0.4, 0.6 and 1.0, and two crack depths of a/t = 0.2 and 0.4. Young's modulus E and Poisson's ratio were assumed to be 205,800MPa and 0.3, respectively. Figs. 8(a), (b)

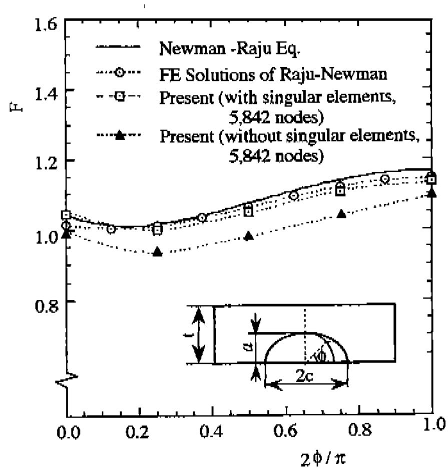

(a) a/c= 0.6, a/t= 0.4

Fig.8 Comparison of present S.I.F. with Newman-Raju solutions

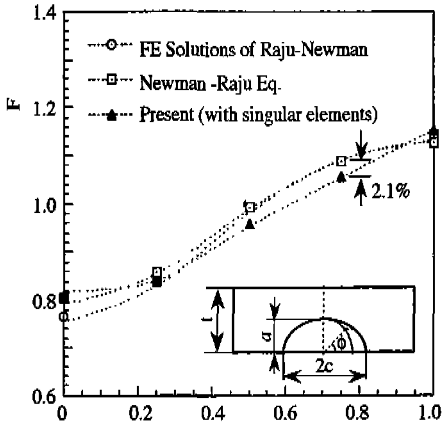

(b) $a/c=0.4$, $a/t=0.2$

Fig.8 Comparison of present S.I.F. with Newman-Raju solutions

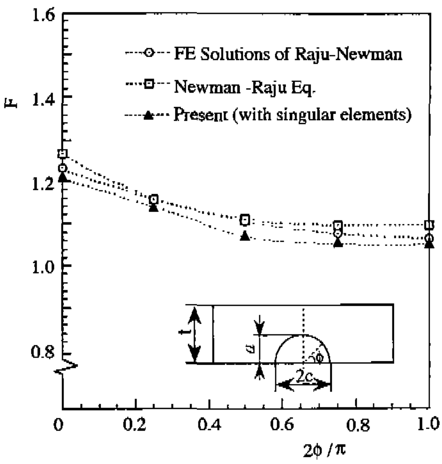

(c) $a/c=1.0$ $a/t=0.4$

Fig.8 Comparison of present S.I.F. with Newman-Raju solutions

and (c) show the comparison between the present solutions and Newman-Raju's solutions[5,12] for single crack configuration. The SIF K for this crack configuration can be often expressed as :

$$K = \sigma\sqrt{\pi a/Q}\ F(a/c, \phi, a/t) \tag{2}$$

where Q is the squared complete elliptical integral of the second kind, and its approximate form is given as :

$$Q = 1 + 1.464\left(\frac{a}{c}\right)^{1.65} \tag{3}$$

It can be seen from the figures that the present results using the singular elements agree well with Raju-Newman's solutions within 2 to 3% difference.

Fig. 9 shows the measured processing time of a whole process plotted against the total number of nodes. These are also measured on a popular engineering workstation, SUN SparcStation 10. Among a whole process, the interactive operations to be done by a user, i.e. the definition of a geometry model, the designation of local node patterns and the assignment of material properties and boundary conditions are performed in about 2 minutes. The other processes are fully automatically performed.

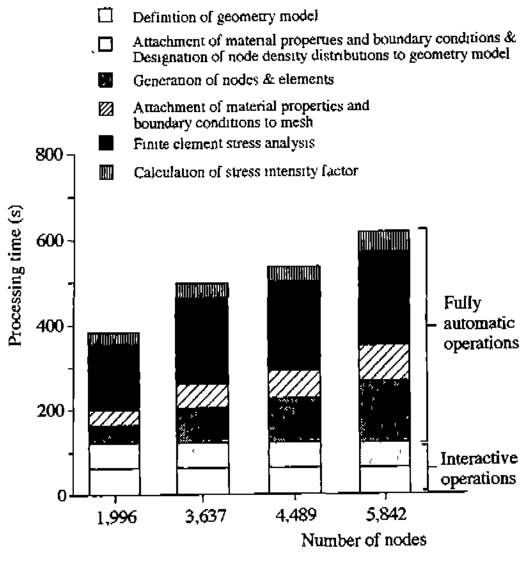

Fig.9 Processing time vs. number of nodes for the analysis of a plate with a semi-elliptical surface crack

4.2 Analyses of Two Identical Surface Cracks in Plate

Next, the present system is applied to solve the SIFs of two identical surface cracks located closely in a plate subjected to uniform tension. Fig. 10 shows a typical FE mesh with 5,160 elements and 9,236 nodes. In this problem, the same three node patterns as in the previous problem were used. Only the special node pattern for a semi-elliptical surface crack is slightly shifted in the width direction of the plate. The mesh in Fig. 10 can be easily created through the same interactive operations as in the previous problem. Nodes and elements are generated in about 2 minutes and in about 40 seconds, respectively, in the computer environment previously mentioned.

To examine interaction effects of two identical surface cracks, the FE analyses are performed for the following crack configurations :

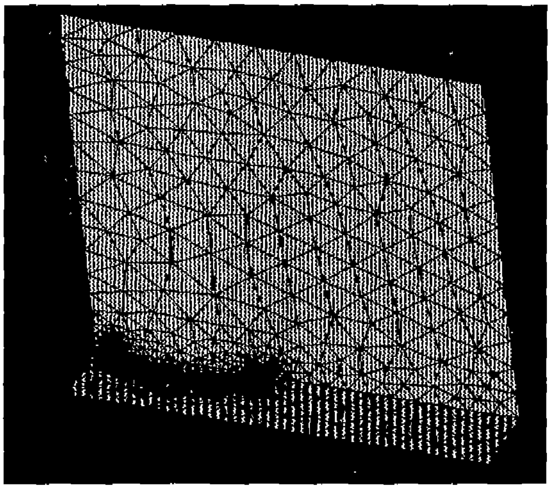

Fig.10 A typical mesh of a quarter portion of a plate with two identical surface cracks(5,160 elements, 9,236 nodes)

$$b/c = h/c = 6.0$$
$$a/t = 0.4, 0.6$$
$$d/c = 0.25,\ 0.5,\ 1.0$$

Fig. 11(a) and (b) show the distributions of the SIF along crack front for different aspect ratios and crack distances. For the purpose of comparison, the analysis results for d/c = 0.25 and 0.5 using the line-spring method of ABAQUS program

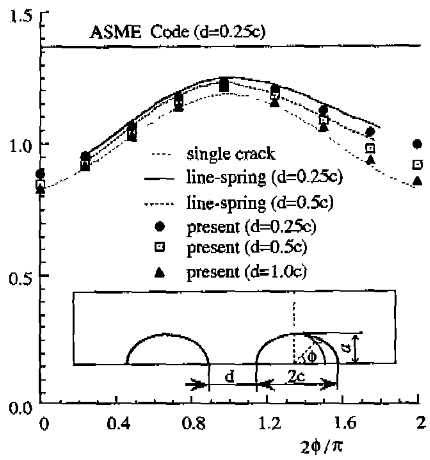

(a) $a/c = 0.4$

Fig.11 Stress intensity factor for two identical surface cracks in a plate

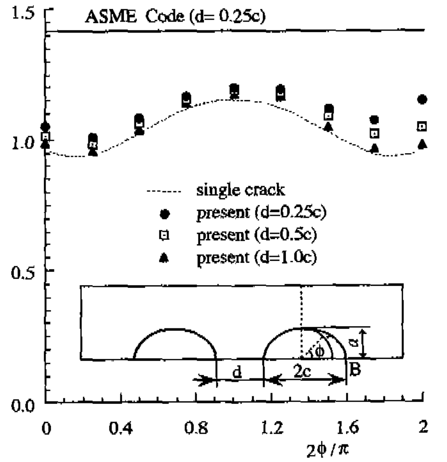

(b) $a/c = 0.6$

Fig.11 Stress intensity factor for two identical surface cracks in a plate

are shown in Fig. 11(a). It can be seen from Fig. 11(a) that the present solutions agree with those by the line-spring method within 5% difference. The figures clearly show that no significant interaction effects are observed when d/c ratio reaches 1, and that the SIF increases significantly near the inner tips of the surface crack when both cracks approach. It should be also noted here that interaction effects on the SIF at the deepest point are negligible even though d/c is 0.25. In ASME Boiler and Pressure Vessel Code, Section XI, Appendix A [18], two adjacent cracks are simply regarded as a single large crack whose depth is the same as that of the deeper original crack, i.e. α and whose length is the same as the distance between the outer tips of the two original cracks, i.e. (4c + d). The SIF for the simplified large crack at the deepest point is shown in Fig. 11(a) and (b) for the purpose of comparison. It can be clearly seen from the figures that the ASME code gives a conservative result for two adjacent cracks problems. These phenomena are in good agreement with those obtained by the body force method[19] and the line spring method[20].

5. Conclusions

A novel automated system for analyzing the SIFs of 3D cracks was developed in the present study. The automatic FE mesh generation technique based on the fuzzy knowledge processing and the computational geometry techniques were integrated in the system, together with one of commercial FE programs. Here interactive operations to be done by a user can be performed in a few minutes even for complicated problems. The other processes are fully automated being able to be performed in several minutes in a popular engineering workstation environment. The results clearly show that when the cracks approach to each other, the SIF at the inner tips of the surface crack significantly increases, but that at the deepest point it does not change so much. Such interaction effects appear more significantly in the smaller crack. ASME Boiler and Pressure Vessel Code, Section XI, Appendix A gives a conservative SIF for two identical surface cracks.

Acknowledgment

This research was supported by Research Fund of Kyonggi University. The author really appreciate the support.

References

1. Wilson, W. K. and Thompson, D. G., "On the Finite Element Method for Calculating Stress Intensity Factors for Cracked Plates in Bending", Engineering Fracture Mechanics, Vol. 3, pp. 97 - 102, 1971.
2. Tracey, D. M., "Finite Elements for Three-Dimensional Elastic Crack Analysis", Nuclear Engineering and Design, Vol. 26, pp. 282 - 290, 1974.
3. Chow, C. L. and Lau, K. J., "On the Finite Element Method for Calculating Stress Intensity Factors with a Modified Elliptical Model", International Journal of Fracture, Vol. 12, pp. 59 - 69, 1976.
4. Blackburn, W. S. and Hellen, T. K., "Calculation of Stress Intensity Factors in Three Dimensions by Finite Element Methods", International Journal for Numerical Methods in Engineering, Vol. 11, pp. 211 - 229,1977.
5. Raju, I. S. and Newman, J. C, "Stress-Intensity Factors for a Wide Range of Semi-Elliptical Surface Cracks in Finite-Thickness Plates", Engineering Fracture Mechanics, Vol. 11, pp. 817 - 829, 1979.
6. Chan, S. K. et al., "On the Finite Element Method in Linear Fracture Mechanics", Engineering Fracture Mechanics, Vol. 2, pp. 1 - 17, 1970.
7. Parks, D. M., "A Stiffness Derivative Finite Element Technique for Determination of Crack Tip Stress Intensity Factors", International Journal of Fracture, pp. 487 - 502, 1974.

8. Yagawa, G. and Nishioka, T., "Finite Element Analysis of Stress Intensity Factors for Plane Extension and Plate Bending Problems", International Journal of Numerical Method in Engineering, Vol. 14, pp. 727 - 740, 1979.
9. Barsoum, R. S., "Application of Quadratic Isoparametric Finite Elements in Linear Fracture Mechanics", International Journal of Fracture, Vol. 10, pp. 603 - 605, 1974.
10. Barsoum, R. S., "Further Application of Quadratic Isoparametric Finite Elements to Linear Fracture Mechanics of Plate Bending and General Shells", International Journal of Fracture, Vol. 11, pp. 167 - 169, 1974.
11. Joon-Seong Lee et al., "Automatic Mesh Generation for Three-Dimensional Structures Consisting of Free-Form Surfaces", The Korea Society of CAD/CAM Engineers, Vol. 1, pp. 65-75, 1996.
12. Newman, J. C. and Raju, I. S., "An Empirical Stress-Intensity Factor Equation for the Surface Crack", Engineering Fracture Mechanics, Vol. 15, pp. 185-192, 1981.
13. Chiyokura, H., "Solid Modeling with DESIGNBASE : Theory and Implementation", Addition - Wesley, 1988.
14. Joon-Seong Lee, "Automated CAE System for Three-Dimensional Complex Geometry", The Doctoral Thesis, The University of Tokyo, 1995.
15. Asano, T., "Practical Use of Bucketing Techniques in Computational Geometry", Computational Geometry, North-Holland, pp. 153 - 195, 1985.
16. Watson, D. F., "Computing the n-Dimensional Delaunay Tessellation with Application to Voronoi Polytopes", The Computer Journal, Vol. 24, pp. 162 - 172, 1981.
17. Sloan, S. W., "A Fast Algorithm for Constructing Delaunay Triangulation in the Plane", Advances in Engineering Software, Vol. 9, pp. 34 - 55, 1987.
18. ASME, ASME Boiler and Pressure Vessel Code, Section XI, Appendix A, 1989.
19. Murakami, Y. and Nisitani, H., "Stress Intensity Factors of Twin Surface Cracks in Semi-Infinite Plate", Transactions of the Japan Society of Mechanical Engineers, (in Japanese), Vol. 47A, pp. 295 - 303, 1981.
20. Miyoshi, T. and Shiratori, M., "Study on Stress Intensity Factors of Closely Located or Partly Overlapped Twin Surface Cracks",Transactions of the Japan Society of Mechanical Engineers, (in Japanese), Vol. 50A, pp. 477 - 482, 1984.